

1 **Depth-related patterns in microbial community responses to complex organic matter in**
2 **the western North Atlantic Ocean**

3 Sarah Brown^{a*}, John Paul Balcombe^{b,c}, Adrienne Hoarfrost^{b,d}, Sherif Ghobrial^b, Carol Arnosti^b

4

5 ^a Environment, Ecology, and Energy Program, University of North Carolina at Chapel Hill,
6 Chapel Hill, North Carolina, USA, 27599

7 ^b Department of Earth, Marine and Environmental Sciences, University of North Carolina at
8 Chapel Hill, Chapel Hill, North Carolina, USA, 27599

9 ^c Current address: HADAL and Nordcee, Department of Biology, University of Southern
10 Denmark, Campusvej 55, 5230

11 ^d Current address: Dept. of Marine Sciences, University of Georgia, Athens, Georgia, USA,
12 30602

13

14 *Correspondence to:* Sarah Brown (sbrown21@live.unc.edu)

15

16 *Keywords: microbial biogeography, enzyme activities, peptidase, polysaccharide hydrolase,*
17 *biological pump, organic matter degradation*

18

19

20

21

22

23

24 **Abstract**

25 Oceanic bacterial communities process a major fraction of marine organic carbon. A substantial
26 portion of this carbon transformation occurs in the mesopelagic zone, and a further fraction fuels
27 bacteria in the bathypelagic zone. However, the capabilities and limitations of the diverse
28 microbial communities at these depths to degrade high molecular weight (HMW) organic matter
29 are not well constrained. Here, we compared the responses of distinct microbial communities
30 from North Atlantic epipelagic (0-200 m), mesopelagic (200-1,000 m), and bathypelagic (1,000-
31 4,000 m) waters at two open ocean stations to the same input of diatom-derived HMW
32 particulate and dissolved organic matter. Microbial community composition and functional
33 responses to the input of HMW organic matter – as measured by polysaccharide hydrolase,
34 glucosidase, and peptidase activities – were very similar between the stations, which were
35 separated by 1370 km, but showed distinct patterns with depth. Changes in microbial community
36 composition coincided with changes in enzymatic activities: as bacterial community composition
37 changed in response to the addition of HMW organic matter, the rate and spectrum of enzymatic
38 activities increased. In epipelagic mesocosms, the spectrum of peptidase activities became
39 especially broad and glucosidase activities were very high, a pattern not seen at other depths,
40 which, in contrast, were dominated by leucine aminopeptidase and had much lower peptidase
41 and glucosidase rates in general. The spectrum of polysaccharide hydrolase activities was
42 enhanced particularly in epipelagic and mesopelagic mesocosms, with fewer enhancements in
43 rates or spectrum in bathypelagic waters. The timing and magnitude of these distinct functional
44 responses to the same HMW organic matter varied with depth. Our results highlight the
45 importance of residence times at specific depths in determining the nature and quantity of
46 organic matter reaching the deep sea.

47 **1. Introduction**

48 Heterotrophic microbial communities play a key role in global biogeochemical cycles by
49 processing up to 50% of the primary productivity produced by phytoplankton in the ocean
50 (Azam, 1998). Much of this organic matter is quickly consumed, transformed, and remineralized
51 in the upper ocean, while most of the remainder is consumed in the mesopelagic zone (200-1,000
52 m), with only a fraction reaching deeper depths (Wakeham et al., 1997; Benner & Amon, 2015).
53 The organic matter reaching the bathypelagic zone (1,000-4,000 m) typically contains low
54 proportions of chemically characterizable carbohydrates, amino acids, and lipids (Benner &
55 Amon, 2015). However, recent investigations have documented rapid transport of freshly-
56 produced organic matter from the upper ocean to the bathypelagic via fast-sinking particles, thus
57 injecting fresh epipelagic-derived organic matter into the deep (Mestre et al., 2018; Ruiz-
58 González et al., 2020; Poff et al., 2021). The extent to which this organic matter is transformed
59 and remineralized once reaching meso- and bathypelagic zones is ultimately determined by the
60 metabolic capabilities of the heterotrophic microbial communities present at these depths.

61 A key step in microbial remineralization of complex high molecular weight (HMW)
62 particulate and dissolved organic matter is its initial hydrolysis to pieces small enough for
63 cellular uptake (Weiss et al., 1991; Arnosti, 2011). Proteins and polysaccharides, which account
64 for the majority of HMW organic matter and are preferentially utilized by bacteria (Amon et al.,
65 2001; Hedges et al. 2001), require distinct, structurally specific extracellular enzymes in order
66 for hydrolysis to occur. The specific capabilities and limitations of natural microbial
67 communities, particularly those in the meso- and bathypelagic, to enzymatically hydrolyze this
68 HMW organic matter are not well-defined, however. Previous studies examining the response of
69 microbial communities to organic matter addition have typically focused on epipelagic water

70 communities, often using a mixture of both low- and high-molecular weight material (e.g., Beier
71 et al. 2015; Luria et al., 2017) to examine community responses. Moreover, the studies that have
72 measured the enzymatic responses of deep ocean communities have relied for the most part on a
73 few small substrate proxies to assess exo-acting (terminal-unit cleaving) enzyme activities (e.g.,
74 Baltar et al., 2010; Sebastián et al., 2021); these substrate proxies do not yield information about
75 the endo-acting (mid-chain cleaving) enzymes essential for degradation of HMW organic matter.

76 As an alternative, the activities of endo-acting enzymes can be measured using
77 fluorescently-labeled polysaccharides (Arnosti 2003) that can probe structure-related differences
78 in polysaccharide hydrolase activities. Such studies have revealed considerable differences in the
79 rate and spectrum of enzyme activities with location and depth in the ocean, with the spectrum of
80 substrates hydrolyzed typically decreasing with depth (Steen et al., 2012; Hoarfrost & Arnosti,
81 2017; Balmonte et al., 2018). Distinct spatial- and depth-related patterns in endopeptidase
82 activities have also been found to exist (Balmonte et al. 2021). These patterns coincide with
83 patterns in the depth-stratification of microbial taxa, genes, and metabolic potential (DeLong et
84 al., 2006; Sunagawa et al., 2015; Guerrero-Feijóo et al., 2016). Together, these results suggest
85 that microbial communities at different depths and locations vary considerably in their abilities
86 to initiate the remineralization of HMW organic matter.

87 As an initial investigation of the enzymatic response of spatially-distinct microbial
88 communities to complex organic matter, we previously added moderate quantities of HMW
89 particulate and dissolved organic matter to epipelagic water and bottom water collected at a shelf
90 station and at an offshore station in the western North Atlantic Ocean. Epipelagic and bottom
91 water communities from a shelf and an open ocean station rapidly responded to HMW organic
92 matter addition, with greater enhancements of rates and a broader spectrum of enzyme activities

93 in communities from the shelf and from epipelagic water relative to the offshore bottom water
94 (Balmonte et al., 2019). Nonetheless, a distinct enhancement in enzyme activities measurable in
95 bathypelagic water from a depth of 4594 m demonstrated that an active heterotrophic community
96 could respond in comparatively short order to an input of HMW organic matter. This initial
97 assessment showed that microbial communities at a shelf and an offshore station responded to an
98 addition of complex HMW organic matter, but the nature of that enzymatic response differed in
99 some key respects. Epipelagic communities, both on the shelf and offshore, responded with
100 higher rates and a broader spectrum of enzymatic activities, while the bottom water community
101 offshore did not exhibit the same breadth of enzymatic activities. Moreover, the bottom water
102 community took longer to respond to the addition of HMW organic matter, and exhibited lower
103 rates of enzymatic hydrolysis than the epipelagic and the shelf bottom water communities.

104 In order to better define the potential and possible enzymatic limitations of open ocean
105 microbial communities, in the present study we sought to determine with greater resolution the
106 depth-gradients in community function and composition, and to determine the extent to which
107 our previous (single-station) open-ocean results apply across larger spatial gradients. We
108 therefore selected two open-ocean stations 1370 kilometers apart, where we investigated organic
109 matter transformation processes in the mesopelagic ocean, where substantial amounts of the
110 organic matter sinking from the epipelagic is remineralized (Wakeham et al., 1997; Benner &
111 Amon, 2015), and compared these results with transformation processes in the epipelagic and
112 bathypelagic ocean. We added moderate quantities (658 μM) of particulate and HMW dissolved
113 organic matter derived from *Thalassiosira weissflogii*, a widespread, abundant diatom (Hartley et
114 al., 1996), to triplicate mesocosms from each depth, and tracked microbial community responses
115 and enzyme activities associated with metabolism of two major classes of marine organic matter,

116 polysaccharides and proteins. By carrying out same experiments at two open-ocean stations, one
117 in the Gulf Stream and one in the Sargasso Sea, we investigated the extent to which spatially-
118 separated, depth-stratified microbial communities may be functionally redundant – or not – in
119 terms of their abilities to hydrolyze the same complex organic matter.

120

121 **2. Materials and methods**

122 ***2.1. Sample sites and sample collection***

123 Water was collected aboard the R/V *Endeavor* in July 2016 at two locations in the western North
124 Atlantic Ocean: Stn. 12 (36° 0'12.12"N, 73° 8'38.46"W), with surface waters in the Gulf Stream,
125 and Stn. 16 (35°59'43.20"N, 58° 2'40.80"W), located in the North Atlantic Gyre (Fig. S1). We
126 focused on epipelagic, mesopelagic (at the oxygen minimum zone, identified from the CTD
127 profile), and bathypelagic water (bottom water), corresponding to depths of 2.5 m, 850 m, and
128 3,660 m at Stn. 12 and 3.5 m, 875 m, and 5,050 m at Stn. 16, respectively. Water was transferred
129 from the Niskin bottles to 20L carboys (acid-washed and rinsed, then rinsed again with sample
130 water prior to filling). Each carboy was filled from a separate Niskin bottle for biological
131 replicates. Triplicate carboys from each depth were amended with moderate (25 mg L⁻¹)
132 quantities of material isolated from *Thalassiosira weissflogii*, corresponding to approximately
133 658 μM of HMW particulate + dissolved organic carbon (see below, and Balmonte et al., 2019).
134 One unamended carboy from each depth served as an incubation control. Carboys were stored in
135 the dark at in-situ or near in-situ temperatures: samples from the epipelagic and mesopelagic
136 were incubated at 21°C, and bottom water samples were incubated at 4°C (Table 1). At each
137 subsampling timepoint (0, 2, 7, and 16 d after the addition of HMW substrate), the carboys were
138 mixed, and subsamples for measurements of cell counts, bacterial production, peptidase and

139 glucosidase activities, and bacterial community composition were collected. Incubations to
 140 measure polysaccharide hydrolase activities were initiated at the 16 d timepoint (see below).

141
 142 **Table 1.** *Sampling depth, in-situ characteristics, and incubation temperatures of water collected*
 143 *for mesocosms at each station and depth.*

	Sampling Depth (m)		In-situ Temp. (°C)		In-situ Salinity (PSU)		In-situ Oxygen (mL/L)		HMW-OM Incub. Temp. (°C)		Enzyme Incub. Temp. (°C)	
	Stn 12	Stn 16	Stn 12	Stn 16	Stn 12	Stn 16	Stn 12	Stn 16	Stn 12	Stn 16	Stn 12	Stn 16
Epipelagic	2.5	3.5	25.3	25.0	36.3	36.4	4.8	4.8	21	21	21	21
Mesopelagic	850	875	10.5	10.5	35.3	35.3	3.1	3.2	21	21	12	12
Bathypelagic	3,660	5,050	2.0	2.0	34.9	34.9	5.8	5.7	4	4	4	4

144
 145 **2.2. High molecular weight organic matter preparation**

146 A HMW substrate was prepared from the diatom *Thalassiosira weissflogii* (Instant Algae, Reed
 147 Mariculture), as described in Balmonte et al. (2019). In brief, frozen and thawed cells were
 148 homogenized with a tissue grinder, dialyzed in a 10 kD membrane (SpectraPor), and the retentate
 149 (HMW dissolved organic matter plus particulate organic matter) was lyophilized, autoclaved,
 150 and lyophilized again. The final HMW *Thalassiosira weissflogii* substrate had a total
 151 carbohydrate concentration of 6.15% and a C:N ratio of 6:1 (Balmonte et al. 2019).

152
 153 **2.3. Bacterial productivity**

154 Bacterial productivity was measured aboard ship according to the methods of Kirchman et al
 155 (1985, 2001). Samples were incubated in the dark at in-situ temperature between 12 and 24 h.
 156 Bacterial protein production was calculated from leucine incorporation rates using the equation
 157 of Simon and Azam (1989), and bacterial carbon production was determined by multiplying
 158 bacterial protein production by 0.86 (Simon and Azam, 1989; Kirchman, 2001).

160 **2.4. Enzymatic hydrolysis measurements**

161 Peptidase and glucosidase activities were measured immediately after the addition of HMW
162 organic matter to the amended carboys, as well as 2, 7, and 16 d post-amendment. These
163 activities were measured using small substrates (glucose, leucine, or peptides) labeled with 4-
164 methyl-coumaryl-7-amide (MCA) or methylumbelliferone (MUF). Exo-acting (terminal-unit
165 cleaving) glucosidase activities were measured with MUF- α - and - β -glucose, and leucine-MCA
166 was used to measure exo-peptidase activities, after the approach of Hoppe (1983). MUF- α - and -
167 β -glucose measure the activities of α - and - β -glucosidases, respectively, which are exo-acting
168 enzymes that hydrolyze terminal glucose units that are initially linked to other molecules in an α -
169 or - β -orientation, respectively. Endopeptidase activities were measured with boc-gln-ala-arg-
170 MCA (QAR, using one-letter amino acid abbreviations) and N-t-boc-phe-ser-arg-MCA (FSR)
171 for trypsin activities, while ala-ala-phe-MCA (AAF) and N-succinyl-ala-ala-pro-phe-MCA
172 (AAPF) were used to measure chymotrypsin activities. Activities were measured in triplicate
173 using a plate reader, following Balmonte et al. (2019), using substrate concentrations of 150 μ M,
174 a concentration based on substrate saturation curves of leucine aminopeptidase and β -glucosidase
175 in Stn. 9 epipelagic waters (76° 36' 6.12"N, 34° 36' 6.552"W). The fluorescence of autoclaved
176 seawater with substrate (controls), and live seawater with no substrate (blanks), was also
177 measured. Samples were incubated close to in-situ temperature, and measured at multiple
178 timepoints – at 0, 6, 12, 18, 24, 36, and 48 hours. Fluorescence readings were converted to
179 activities using a standard curve of free fluorophores (MCA, MUF) in seawater. Hydrolysis rates
180 were averaged over the first 48 hours of measurements for each sampling day.

181 Polysaccharide hydrolase activities were measured using six fluorescently-labeled
182 polysaccharides (pullulan, laminarin, xylan, fucoidan, arabinogalactan, and chondroitin sulfate;

183 Arnosti 2003), chosen for their varying structural complexities and abundances in the ocean. For
184 example, laminarin, a storage glucan found in phytoplankton, including diatoms, is highly
185 abundant in the ocean (Alderkamp et al. 2007; Becker et al., 2020; Vidal-Melgosa et al., 2021),
186 and plays a substantial role in oceanic carbon cycling as it is rapidly hydrolyzed by marine
187 bacteria (e.g., Arnosti et al. 2011; Hoarfrost & Arnosti 2017; Balmonte et al. 2021). More
188 complex polysaccharides, including arabinogalactan, a polysaccharide found in green
189 microalgae, and fucoidan, a cell wall polysaccharide produced by brown algae that is also
190 present in diatom exudates (Vidal-Melgosa et al. 2021), are less readily degraded by marine
191 bacteria, and may persist in the ocean for longer periods of time (Sichert et al., 2020; Vidal-
192 Melgosa et al., 2021). Additionally, marine bacteria capable of degrading the chosen
193 polysaccharides have been identified, including bacteria in the classes *Gammaproteobacteria*
194 and *Bacteroidia* that consume laminarin (Alderkamp et al., 2007; Teeling et al., 2012; Vidal-
195 Melgosa et al., 2021), while *Verrucomicrobia* are capable of fucoidan hydrolysis (Sichert et al.,
196 2020). The other polysaccharides (pullulan, xylan, and chondroitin sulfate) are known to be
197 marine-derived, and/or their hydrolysis of these substrates is carried out by marine bacteria (e.g.,
198 Arnosti & Repeta 1994; Wegner et al. 2013; Araki et al. 2000.)

199 Measurements of these six polysaccharides were initiated in water from the amended and
200 unamended mesocosms 16 d after the start of the experiment, an initial time-lag that should
201 allow the microbial community in amended mesocosms to respond – via enzyme expression as
202 well as shifts in community composition – to the addition of *Thalassiosira*-derived material.
203 Incubations were carried out after Balmonte et al. (2019). All incubations were kept in the dark
204 at in-situ temperatures. Subsamples were collected 0, 2, 5, 10, 17, and 30 d after polysaccharide
205 addition. Hydrolysis rates were calculated as previously described (Arnosti, 2003). Note that all

206 enzymatic hydrolysis rates – polysaccharide hydrolase as well as peptidase – should be
207 considered potential rates, since added substrate is in competition with naturally-occurring
208 substrates for enzyme active sites.

209

210 ***2.5. 16S rRNA sequencing and phylogenetic analysis***

211 To analyze bacterial community composition, 250 to 2,500 mL of seawater from each carboy
212 was filtered using a vacuum pump through a 0.2 µm pore size, 47 mm diameter Whatman
213 Nuclepore Track-Etched Membrane filter (see Supplemental Information Table S1 for volumes
214 filtered). Samples were stored at -80°C until analysis. At least one quarter of each filter was cut
215 with a sterile razor blade and used for DNA extraction. Analysis of sample duplicates (i.e.,
216 pieces of different filters from the same sample) and/or filter duplicates (duplicate quarters of a
217 single filter) were also analyzed for a select number of samples. DNA was extracted using a
218 DNeasy PowerSoil Kit (Qiagen) according to manufacturer protocol. The 16S rRNA gene was
219 sequenced at the UNC Core Microbiome Facility with Illumina MiSeq PE 2x250. Amplification
220 of the hypervariable regions V1 and V2 of the 16s rRNA gene was conducted using the 8F (5'-
221 AGA GTT TGA TCC TGG CTC AG-3') and 338R (5'-GC TGC CTC CCG TAG GAG T-3')
222 primers with the Illumina-specific forward primer overhang adapter (5'- TCG TCG GCA GCG
223 TCA GAT GTG TAT AAG AGA CAG-3') and reverse overhang adapter (5'- GTC TCG TGG
224 GCT CGG AGA TGT GTA TAA GAG ACA G-3').

225 Sequences were imported into QIIME2 for analysis (version 2017.12; <https://qiime2.org>;
226 Bolyen et al., 2019), where, after demultiplexing, primers were trimmed using cutadapt (Martin,
227 2011) and denoising, dereplicating, filtering of chimeras and singletons, and merging of paired
228 end reads was conducted using DADA2 (Callahan et al., 2016). OTUs were clustered and picked

229 *de-novo* at a sequence similarity of 97% using vsearch (Rognes et al., 2016). Taxonomy was
230 assigned using a Naïve Bayes classifier that was trained using reference sequences with the 8F
231 and 338R primers from the Silva database (version 128; Pruesse et al., 2007). Chloroplasts were
232 removed, and samples were rarefied to an even sampling depth of 10,810 sequences using the
233 phyloseq package in R (version 1.19.1; McMurdie & Holmes, 2013). Raw sequence files can be
234 accessed on the NCBI Sequence Read Archive under the accession number PRJNA480640.

235

236 ***2.6. Statistical analyses***

237 To test for differences in bacterial productivity, bacterial abundance, polysaccharide hydrolase
238 activities, and peptidase and glucosidase activities between different stations, depths, and
239 treatments over time, ANOVA was performed using the nlme package (version 3.1-131; Pinheiro
240 et al., 2018) in R (R Core Team, 2017). Bacterial abundance, richness, and evenness were log
241 transformed, while bacterial productivity and all enzymatic activities were transformed
242 according to $\ln(x+0.5)$, in order to meet the assumptions of an ANOVA. In each test, station,
243 depth, treatment, and timepoint were considered fixed variables, and mesocosm was considered a
244 random variable. According to ANOVAs, the four-way interaction (between station, depth,
245 treatment, and timepoint) was not significant for bacterial productivity, bacterial abundance, or
246 any of the enzymatic activities, and these were therefore excluded from the ANOVA test.

247 Differences in bacterial community composition were visualized using non-metric
248 multidimensional scaling (NMDS) based on the Bray-Curtis dissimilarity index using the
249 phyloseq package in R (version 1.19.1; McMurdie & Holmes, 2013). To test for differences in
250 bacterial community composition between groups, PERMANOVAs were conducted using the
251 adonis function (vegan) (version 2.4-6; Oksanen et al., 2018) in R. Estimates of richness and

252 evenness of bacterial community composition were calculated in R using the estimate richness
253 function in the phyloseq package (version 1.19.1; McMurdie & Holmes, 2013). To examine the
254 correlation between enzymatic activities and bacterial community composition, Mantel tests
255 using the Pearson correlation method were conducted on the Bray-Curtis dissimilarity index of
256 bacterial community composition and a Euclidean distance matrix computed from peptidase and
257 glucosidase activities using the vegan package in R (version 2.4-6; Oksanen et al., 2018).

258

259 **3. Results**

260 ***3.1. Water mass characteristics***

261 The two stations in the western North Atlantic Ocean, separated by a distance of 1370
262 km, included the same water masses at each depth, based on temperature and salinity
263 characteristics: epipelagic water at both stations was North Atlantic Surface Water, water from
264 the mesopelagic (850 m at Stn. 12; 875 m at Stn. 16) was North Atlantic Central Water, and
265 bathypelagic water at both stations was North Atlantic Deep Water (Talley, 2011; Heiderich &
266 Todd, 2020; Table 1; Supplemental Information Fig. S1, S2). Water mass characteristics in the
267 epi-, meso-, and bathypelagic were substantially different from one another (see Table 1;
268 Supplemental Information Fig. S2) enabling the examination of bacterial communities
269 experiencing distinct environmental conditions at two open ocean stations – one situated within
270 the Gulf Stream, and one located in the Sargasso Sea).

271

272 ***3.2. Peptidase and glucosidase activities***

273 Peptidases hydrolyze peptides and proteins to smaller substrates, whereas glucosidases
274 hydrolyze terminal glucose units from larger molecules. Since peptidase and glucosidase

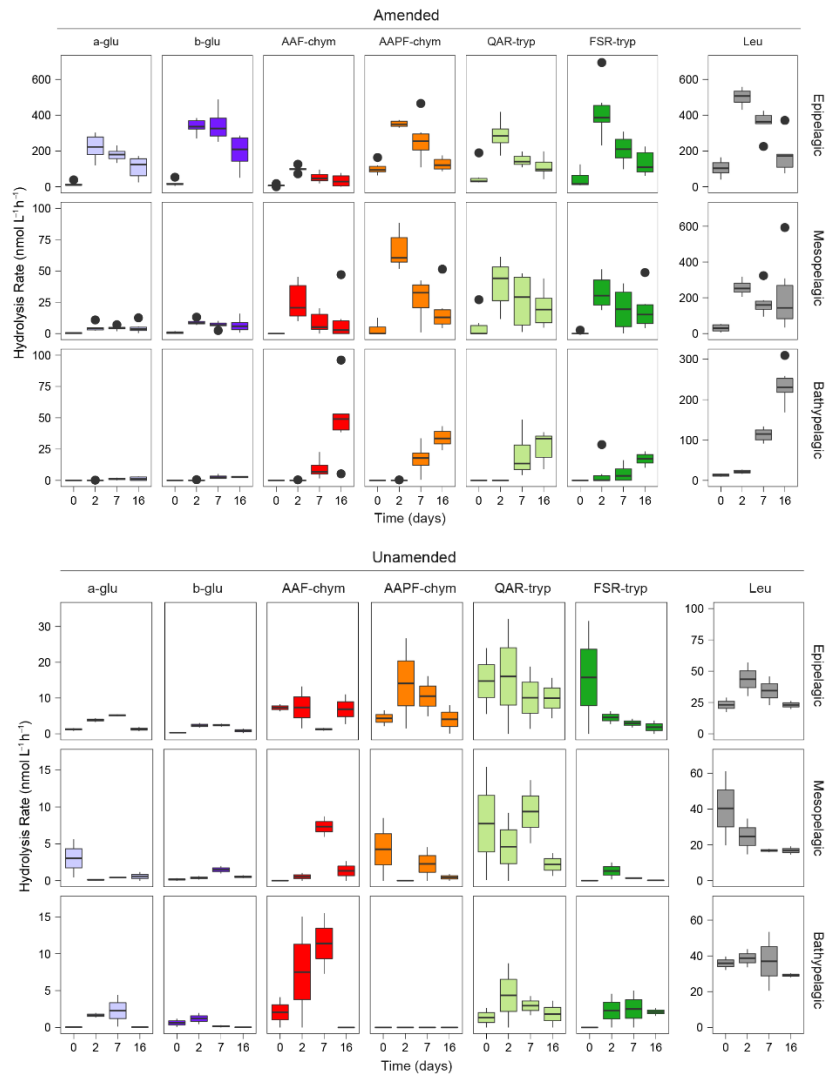
275 activities differed by depth, but not by station in both amended and unamended mesocosms
276 (ANOVA, $p=0.2424$), in the following sections, data from the same depths at the two stations are
277 presented together, yielding two unamended and six amended mesocosms per depth. Data from
278 individual mesocosms are presented in supplemental figures.

279 In unamended epipelagic water mesocosms, all seven peptidase and glucosidase
280 substrates were hydrolyzed at rates higher than in the mesopelagic or bathypelagic waters (Fig.
281 1; Supplemental Information Fig. S3); in epipelagic waters, endopeptidase activities (i.e., AAF-
282 chymotrypsin, AAPF-chymotrypsin, QAR-trypsin, and FSR-trypsin) were also a higher fraction
283 of summed activity than at other depths (Supplemental Information Fig. S3). Bathypelagic
284 waters were dominated by leucine-MCA and AAF-chym activities; no AAPF-chym activity was
285 detected (Fig. 1; Supplemental Information Fig. S3).

286 Addition of HMW organic matter led to a substantial increase in the rates and spectrum
287 of peptidase and glucosidase activities (Fig. 1) (ANOVA, $p<0.0001$). The responses of the six
288 amended mesocosms per depth, drawn from six different Niskin bottles across two different
289 stations, were very similar (Supplemental Information Fig. S3). The timing of these responses to
290 added organic matter varied with depth, however, suggesting that depth had a stronger influence
291 on enzymatic responses than location. At t_0 , immediately after HMW organic matter addition,
292 hydrolysis rates and patterns in amended mesocosms were similar to the unamended mesocosms.
293 By the 2 d timepoint, activities had increased by approximately an order of magnitude in the
294 epipelagic mesocosms, and the hydrolysis rates of the substrates became more even. In amended
295 mesopelagic mesocosms, after 2 d all activities were approximately a factor of 5 greater than in
296 unamended mesocosms. However, a shift in enzymatic response to HMW organic matter
297 amendment, defined as the point at which the rates and spectrum of peptidase and glucosidase

298 activities increased significantly, in bathypelagic mesocosms was not observed until 7 d post-
299 addition (Fig. 1; Supplemental Information Fig. S3).

300 The stimulation of specific peptidase and glucosidase activities in amended mesocosms
301 also differed by depth (Fig. 1) (ANOVA, $p < 0.0001$), pointing to further depth-related functional
302 capabilities between epipelagic, mesopelagic, and bathypelagic communities. The amended
303 epipelagic water mesocosms showed particularly high α - and β -glucosidase activities, which
304 accounted for 4% to 47% of the total summed hydrolysis rates, and relatively even peptidase
305 activities (Fig. 1). In contrast, α - and β -glucosidase activities accounted for, at most, ~12% of the
306 total summed hydrolysis rates in mesopelagic mesocosms and only 3.3% of the total summed
307 hydrolysis rates in bathypelagic mesocosms. Mesopelagic and bathypelagic mesocosms were
308 typically dominated by high leucine aminopeptidase activities, although this was most notable in
309 bathypelagic mesocosms (Fig. 1).



310

311 **Figure 1.** Peptidase and glucosidase activities in amended and unamended mesocosms 0, 2, 7,

312 and 16 d after the addition of HMW organic matter to amended mesocosms. Rates are an

313 average between the two stations. Note the difference in scales between the amended and

314 unamended mesocosms. a-glu = α -glucose, b-glu = β -glucose, AAF-chym = AAF

315 (chymotrypsin), AAPF-chym=AAPF (chymotrypsin), QAR-try = QAR (trypsin), FSR-try =

316 FSR (trypsin), and Leu = leucine-MCA.

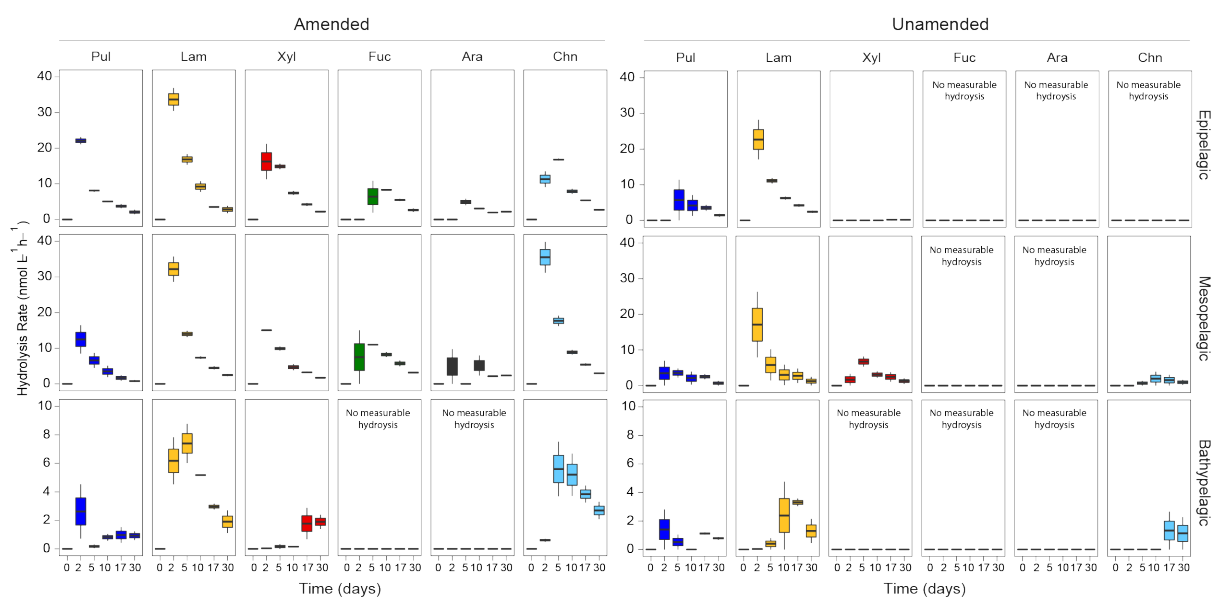
317

318 **3.4. Polysaccharide hydrolase activities**

319 Only a limited range of polysaccharides were hydrolyzed in unamended mesocosms.
320 Laminarin and pullulan were hydrolyzed at all depths and stations. However, fucoidan and
321 arabinogalactan, more complex polysaccharides (see Methods for additional information), were
322 not hydrolyzed at any depth or station in unamended mesocosms (Fig. 2; Supplemental
323 Information Fig. S4). Chondroitin was also hydrolyzed in Stn. 16 mesopelagic and bathypelagic
324 mesocosms, and xylan was hydrolyzed in Stn. 16 epipelagic and mesopelagic mesocosms of both
325 stations (Fig. 2; Supplemental Information Fig. S4). The spectrum of polysaccharide hydrolase
326 activities was therefore broadest in the mesopelagic. The time course over which individual
327 polysaccharides were hydrolyzed also varied by substrate and depth. In unamended epipelagic
328 and mesopelagic mesocosms, laminarinase activities were generally high at the 2 d timepoint;
329 pullulanase activities were detected slightly later, except in Stn. 16 mesopelagic mesocosms,
330 where pullulanase activity was also measurable at 2 d. Xylanase activity was measurable at 2 d
331 (Stn. 12) or at 5 d (Stn. 16) in mesopelagic mesocosms; chondroitin hydrolysis was measurable
332 starting at 5 d at Stn. 16. The unamended bathypelagic mesocosms showed slightly different
333 patterns, with polysaccharide hydrolase activity detectable starting at 2 d at Stn. 16, but only
334 detectable at 17 d at Stn. 12 (Supplemental Information Fig. S4).

335 Polysaccharide hydrolase activities were significantly different between amended and
336 unamended mesocosms (ANOVA, $p < 0.0001$). Addition of HMW organic matter increased the
337 rates, broadened the spectrum, and changed the timepoint at which polysaccharide hydrolase
338 activities were first detected (Fig. 2). All six polysaccharide hydrolase activities were measurable
339 in epipelagic and mesopelagic mesocosms, with the initial timepoint of detection typically at 2 d
340 or 5 d. In amended bathypelagic mesocosms, pullulan, laminarin, and chondroitin hydrolysis
341 were typically initially measured at the 2 d or 5 d timepoints; xylanase activity was usually only

342 detected at the later (17 d or 30 d) timepoints. Maximum polysaccharide hydrolase activities
 343 were significantly lower in amended bathypelagic mesocosms (summed activities lower than 20
 344 $\text{nmol L}^{-1} \text{h}^{-1}$) than in epipelagic and mesopelagic mesocosms (summed activities at or above 50
 345 $\text{nmol L}^{-1} \text{h}^{-1}$) (ANOVA, $p < 0.0001$) (Supplemental Information Fig. S5). In amended
 346 mesocosms, stations did not differ significantly in either the maximum rates (ANOVA, $p =$
 347 0.8401) or the temporal development of polysaccharide hydrolase activities (ANOVA, $p =$
 348 0.7502). Polysaccharide hydrolase activities thus mirror the activities of peptidases and
 349 glucosidases, with depth-related differences in enzymatic activities prevailing over location-
 350 related differences.



351
 352 **Figure 2.** Polysaccharide hydrolase activities in amended and unamended mesocosms, averaged
 353 between stations. The spectrum of substrates (the range of substrates hydrolyzed) was
 354 considerably broader in amended compared to unamended mesocosms. Note that the 0 d
 355 timepoint, when fluorescently-labeled polysaccharide incubations began, was 15 d after the
 356 addition of HMW-OM to amended mesocosms. Note the large difference in scales between epi-
 357 and mesopelagic mesocosms (up to $40 \text{ nmol L}^{-1} \text{h}^{-1}$) and bathypelagic mesocosms (up to 10 nmol

358 $L^{-1} h^{-1}$). *Pul* = pullulan, *Lam* = laminarin, *Xyl* = xylan, *Fuc* = fucoidan, *Ara* = arabinogalactan,
359 *Chn* = chondroitin.

360

361 **3.5. Bacterial protein production**

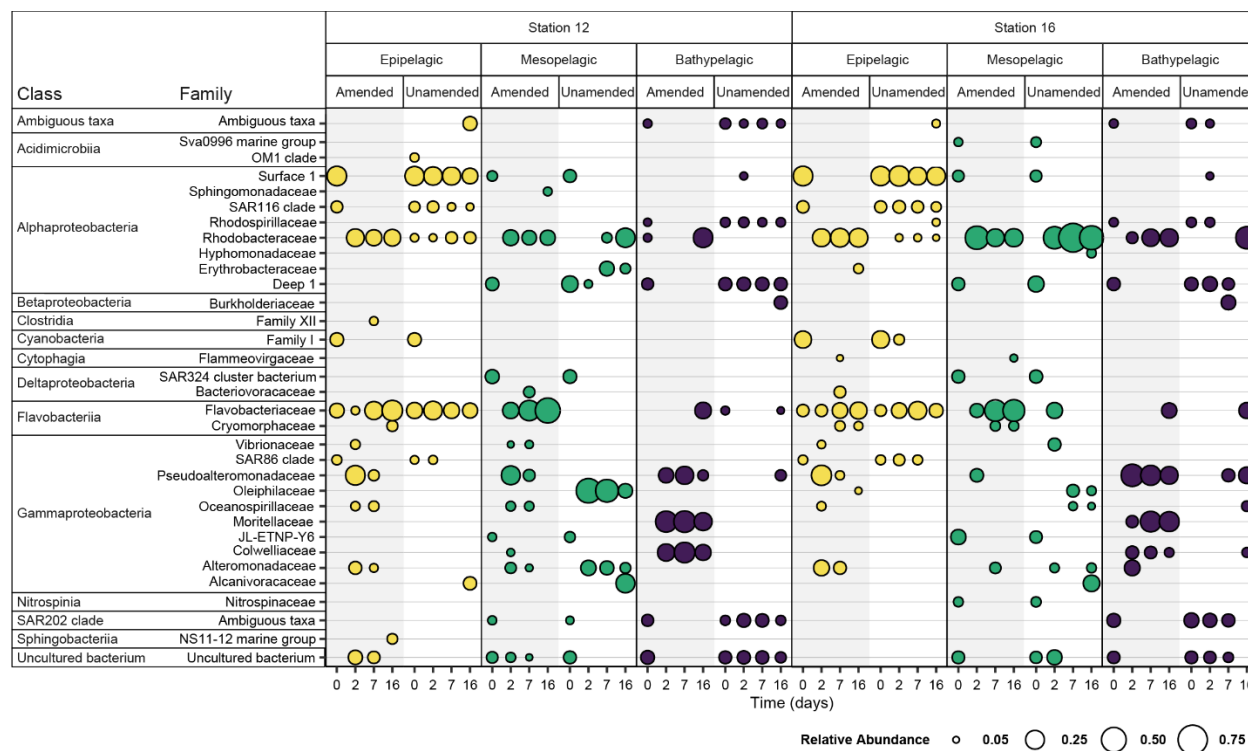
362 In amended epipelagic mesocosms, bacterial protein production was high immediately
363 after addition of HMW organic matter (ca. 150 $\mu\text{M h}^{-1}$), and decreased at subsequent time points
364 (Supplemental Information Fig. S6a). In unamended epipelagic mesocosms, bacterial protein
365 production was initially low, but increased from 20.6 $\mu\text{M h}^{-1}$ in Stn. 12 mesocosms and 99.3 $\mu\text{M h}^{-1}$
366 in Stn. 16 mesocosms to rates above 150 $\mu\text{M h}^{-1}$ at subsequent timepoints. In mesopelagic
367 mesocosms, bacterial protein production increased in both the amended and unamended
368 mesocosms from very low initial levels to much higher levels at later timepoints. In Stn. 16
369 mesocosms, bacterial protein production increased with time in both the amended and
370 unamended mesocosms; in Stn. 12 mesocosms, the patterns were less clear (Supplemental
371 Information Fig. S6a). Bathypelagic amended mesocosms showed detectable bacterial protein
372 production at earlier timepoints than unamended mesocosms, with rates above 50 $\mu\text{M h}^{-1}$ at 7 d.
373 Bacterial protein production varied significantly between mesocosms amended with HMW
374 organic matter and unamended mesocosms (ANOVA, $p = 0.0054$), with changes in protein
375 production displaying distinct trends with depth (ANOVA, $p < 0.0001$).

376

377 **3.6. Bacterial community composition**

378 Initial bacterial communities in epipelagic unamended and amended mesocosms were
379 dominated by *Alphaproteobacteria*, *Cyanobacteria*, *Flavobacteriia*, and *Gammaproteobacteria*,
380 as demonstrated by relative read abundance (Fig. 3; Supplemental Information Fig. S7). In meso-

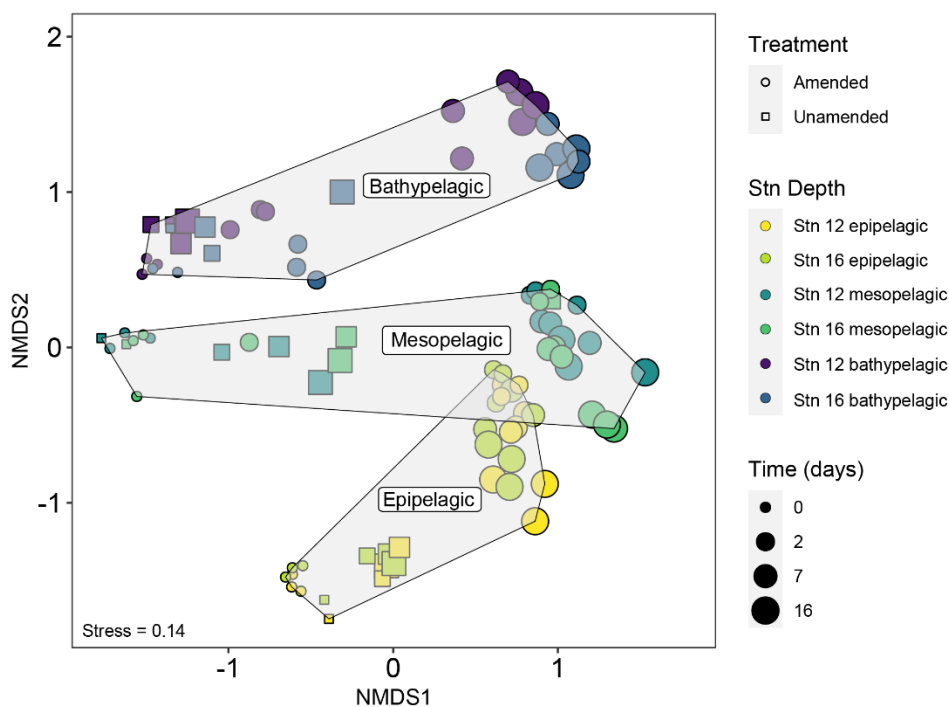
381 and bathypelagic mesocosms, *Alphaproteobacteria*, *Deltaproteobacteria*,
382 *Gammaproteobacteria*, *Flavobacteriia*, and the SAR202 clade dominated initial bacterial
383 communities, although these classes were present in different relative proportions in mesopelagic
384 and bathypelagic mesocosms (Fig. 3; Supplemental Information Fig. S7). As expected, initial
385 (t0) bacterial communities in amended and unamended mesocosms were not significantly
386 different from one another (PERMANOVA, $R^2 = 0.02016$, $p = 0.655$). Distinct bacterial
387 communities were present in mesocosms from different depths (Fig. 4; Supplemental
388 Information Fig. S8), and depth explained the greatest amount of dissimilarity between bacterial
389 communities (PERMANOVA, $R^2 = 0.1968$, $p = 0.001$). Samples from comparable depths
390 clustered together, regardless of their station of origin (shown by non-metric multidimensional
391 scaling (NMDS) based on the Bray-Curtis dissimilarity index; Fig. 4; Supplemental Information
392 Fig. S8). However, samples collected from the same water masses but at different stations still
393 displayed differences in community composition that were statistically significant
394 (PERMANOVA, $R^2 = 0.0190$, $p = 0.001$); we have therefore graphed community composition at
395 each station separately (Fig. 3; Supplemental Information Fig. S7). Duplicate filters, both sample
396 duplicates and filter duplicates from the same depth and station, displayed consistent
397 reproducibility of bacterial community composition: hierarchical clustering showed that
398 duplicates clustered closest together, except in a single case (Supplemental Information Fig. S9).



399
 400 **Figure 3.** Bacterial families with a normalized relative abundance of 5% or more in amended
 401 and unamended mesocosms from each station and depth 0, 2, 7, and 16 d after the addition of
 402 HMW organic matter to amended mesocosms. Amended values are an average of triplicate
 403 amended mesocosms, and the bubble size indicates the relative abundance (%) of each bacterial
 404 family. Note that “Ambiguous taxa” represents those sequences for which the taxonomy did not
 405 meet a consensus when compared to the reference database.

406
 407 Addition of HMW organic matter resulted in distinct shifts in bacterial community
 408 composition, which were evident starting at 2 d (Figs. 3, 4; Supplemental Information Fig. S7).
 409 While initial bacterial communities from the mesopelagic were more compositionally and
 410 phylogenetically similar to bathypelagic communities (Supplemental Information Figs. S7, S10),
 411 after HMW organic matter addition, mesopelagic communities progressively became more
 412 similar to bacterial communities in epipelagic mesocosms. This shift was the result of similar

413 increases in the relative proportions of *Gammaproteobacteria* and *Flavobacteriia*, and a decrease
 414 in the relative proportion of *Alphaproteobacteria*, in amended epipelagic and mesopelagic
 415 mesocosms (Fig. 3; Supplemental Information Fig. S7). Relative read abundances for
 416 *Flavobacteriia* and *Alphaproteobacteria* in bathypelagic mesocosms were notably lower than in
 417 epipelagic and mesopelagic mesocosms, while *Gammaproteobacteria* relative read abundance
 418 was higher. The composition of bacterial communities in unamended mesocosms also shifted
 419 with time, showing evidence of a ‘bottle effect’. However, these compositional shifts were
 420 observed to a lesser extent (Fig. 3; Supplemental Information Fig. S7) and, especially for
 421 bathypelagic mesocosms, occurred at later time points than in their amended counterparts (Fig.
 422 3; Supplemental Information Fig. S7).



423
 424 **Figure 4.** Non-metric multidimensional scaling (NMDS) plot of bacterial community
 425 composition based on the Bray-Curtis dissimilarity index shows that communities were quite
 426 distinct by depth. In later phases of the incubations, however, the amended mesopelagic and

427 *epipelagic mesocosms become more similar to one another. Note also that mesocosms from Stns.*
428 *12 and 16 from a given depth and timepoint – especially for epipelagic and mesopelagic samples*
429 *- remained similar to one another through the course of the incubations.*

430

431 Within the *Gammaproteobacteria*, families that became abundant after addition of HMW
432 organic matter were initially present in very low relative proportions and, in some cases, were
433 not detected during initial timepoints (Supplemental Information Fig. S11). The
434 Gammaproteobacterial families with highest read abundance varied with depth, with taxa in the
435 *Alteromonadaceae*, *Colwelliaceae*, *Oceanospirillaceae*, *Pseudoalteromonadaceae*, and
436 *Vibrionaceae* families becoming abundant in epipelagic and mesopelagic mesocosms, while
437 bathypelagic mesocosms were dominated by taxa in the *Alteromonadaceae*, *Colwelliaceae*,
438 *Moritellaceae*, and *Pseudoalteromonadaceae* families (Supplemental Information Fig. S11).
439 Although members of the *Alteromonadaceae*, *Colwelliaceae*, and *Pseudoalteromonadaceae*
440 were present in amended mesocosms from all depths, their relative proportion varied with depth:
441 the highest relative proportion of *Alteromonadaceae* typically occurred in epipelagic and
442 mesopelagic mesocosms, while *Colwelliaceae* were most abundant in bathypelagic mesocosms;
443 the relative proportion of *Pseudoalteromonadaceae* did not follow a consistent depth-related
444 pattern (Supplemental Information Fig. S11). In some cases, a single genus or OTU within these
445 families became abundant (Supplemental Information Fig. S12, S13); for example, in the
446 *Colwelliaceae* family, an OTU in the genus *Colwellia* became abundant in all amended
447 mesocosms (Supplemental Information Fig. S14).

448 The presence of these gammaproteobacterial families in amended mesocosms contrasts
449 sharply with the dominant families in unamended mesocosms: in epipelagic water unamended

450 mesocosms, the SAR86 clade remained the dominant taxa throughout most timepoints, while the
451 proportion of *Pseudoalteromonadaceae* and *Oceanospirillaceae* remained low. In unamended
452 bathypelagic mesocosms, taxa that were initially highly abundant, such as the *Salinisphaeraceae*,
453 also typically comprised a large proportion of all taxa during subsequent timepoints
454 (Supplemental Information Fig. S11). However, in unamended mesopelagic mesocosms, relative
455 gammaproteobacterial read abundance shifted considerably after the initial timepoint. The taxa
456 that became abundant were present, albeit at low relative abundances, during initial timepoints,
457 and the patterns in the abundance of these taxa differed between stations.

458 While distinct families in the *Gammaproteobacteria* became abundant in water from
459 different depths, the same families in the *Alphaproteobacteria* and *Flavobacteriia* became
460 dominant in all amended mesocosms after t₀, regardless of depth. Within the *Flavobacteriia*,
461 members of the *Flavobacteriaceae* family increased in relative read abundance in all mesocosms
462 after t₀, although they were generally less abundant in bathypelagic mesocosms than in
463 epipelagic and mesopelagic mesocosms (Supplemental Information Fig. S15). The relative
464 proportion of other *Flavobacteriia* families, including the *Cryomorphaceae* and the NS9 Marine
465 Group, decreased over time. The same trend was observed in all unamended mesocosms
466 (Supplemental Information Fig. S15). Although the *Flavobacteriaceae* family became abundant
467 in all amended mesocosms, the dominant *Flavobacteriaceae* genera varied greatly with depth
468 (Supplemental Information Fig. S16). For example, *Polaribacter 4*, although present to some
469 degree in all amended mesocosms, was the most abundant *Flavobacteriaceae* genera in
470 bathypelagic mesocosms, while *Tenacibaculum* was more abundant in epipelagic and
471 mesopelagic mesocosms (Supplemental Information Fig. S16). In the *Alphaproteobacteria*, the
472 *Rhodobacteraceae* became dominant in all amended mesocosms, despite only making up a low

473 relative proportion of *Alphaproteobacteria* families initially (Supplemental Information Fig
474 S16). A shift in the relative proportions of Alphaproteobacterial families occurred after 2 d in
475 epipelagic and mesopelagic mesocosms, and after 7 d in bathypelagic mesocosms, when the
476 *Rhodobacteraceae* became the dominant Alphaproteobacterial family (Supplemental Information
477 Fig. S17). Within the *Rhodobacteraceae* family, bacteria in the genus *Sulfitobacter* became
478 particularly abundant in all amended mesocosms (Supplemental Information Fig. S18).

479 Bacterial richness, evenness, and Shannon diversity typically decreased in all amended
480 mesocosms 2 d after the addition of HMW organic matter; this decrease was greatest in water
481 from the meso- and bathypelagic (Supplemental Information Fig. S6). However, in epipelagic
482 and mesopelagic mesocosms, these decreases in diversity were not significantly different from
483 those in unamended mesocosms (ANOVA, $p > 0.05$ for all, Supplemental Information Table S2).
484 Only in bathypelagic mesocosms were changes in richness, evenness, and diversity significantly
485 different between amended and unamended mesocosms (ANOVA, $p < 0.005$, Supplemental
486 Information Table S2): while richness, evenness, and diversity in amended bathypelagic
487 mesocosms had decreased significantly 2 d after the addition of HMW organic matter, the
488 decrease in these parameters in unamended mesocosms was more gradual, and in some cases
489 even increased or remained relatively consistent (Supplemental Information Fig. S6).

490

491 ***3.7. Relating community composition to enzymatic activities***

492 Successional patterns in bacterial community composition were concurrent with
493 functional changes in enzymatic capabilities. Notable changes in peptidase and glucosidase
494 activities in epipelagic and mesopelagic mesocosms at the 2 d timepoint corresponded with a
495 major shift in bacterial community composition (Figs. 1, 4), with *Gammaproteobacteria* and

496 *Flavobacteriia* becoming highly abundant (Fig. 3). In bathypelagic mesocosms, a shift of similar
497 magnitude was measured 7 d after the addition of HMW organic matter (Fig. 4). Since the
498 unamended mesocosms did not show comparable shifts in enzyme activities or community
499 composition, a major driver of the shifts in amended mesocosms was most likely the addition of
500 HMW organic matter, rather than bottle effects. The relationship between bacterial community
501 composition and peptidase and glucosidase activity in amended mesocosms after 2 d was
502 stronger and of greater significance (Mantel $R = 0.1483$, $p = 0.003$) than in unamended
503 mesocosms and amended mesocosms at t_0 , when the relationship between bacterial community
504 composition and peptidase and glucosidase activity was not significant Mantel $R = 0.0080$, $p = 0.$
505 356).

506

507 **4. Discussion**

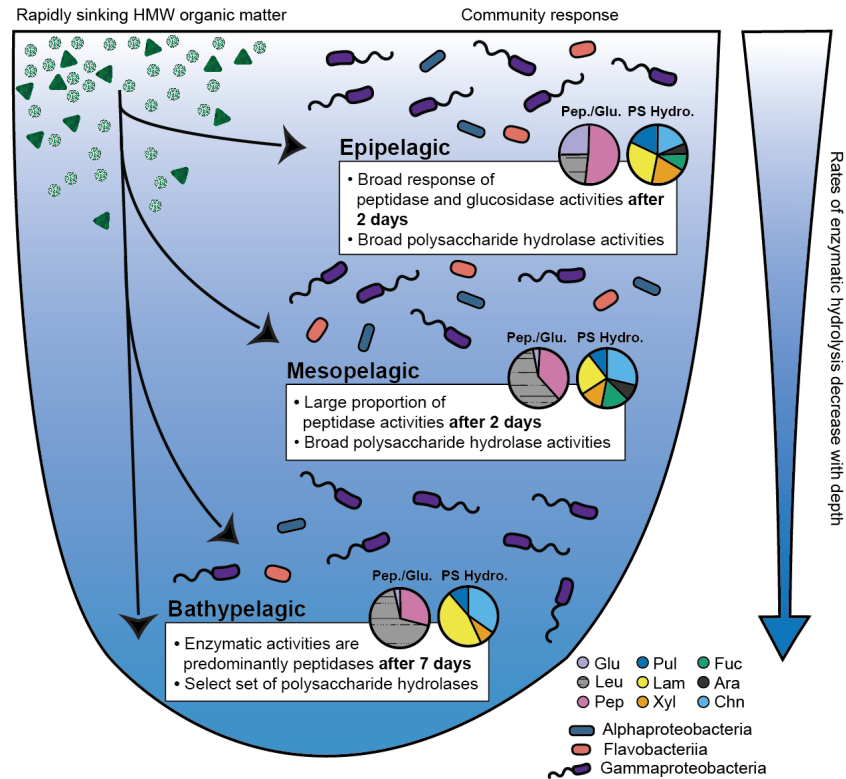
508 Distinct depth-related differences in enzyme function and community composition
509 characterized the epipelagic, mesopelagic, and bathypelagic mesocosms: with increasing depth,
510 the rates and/or spectrum of substrates hydrolyzed decreased, consistent with previous
511 measurements of enzymatic activities in unamended water (Hoarfrost & Arnosti, 2017; Balmonte
512 et al., 2018, Hoarfrost et al., 2019). Addition of HMW organic matter, however, revealed depth-
513 related responses that were not evident in the unamended mesocosms: not only the rates, but also
514 the spectrum of enzyme activities broadened in amended mesocosms, but the extent to which this
515 broader spectrum was measurable varied by depth, with the amended bathypelagic microbial
516 communities in particular showing a less-broad response than their mesopelagic and epipelagic
517 counterparts (Fig. 5).

518 These depth-related functional differences were similar between comparable depths at
519 two stations separated by 1370 km (Supplemental Information Figs. S1, S3, S4). Furthermore,
520 the patterns were also very similar to those measured in epipelagic and bathypelagic mesocosms
521 amended with the same HMW organic matter at a different open ocean station in the western
522 North Atlantic Ocean during the previous year (Balmonte et al. 2019; Stn. 8, water depth 4574
523 m; Supplemental Information Fig. S1). These results suggest that the response of bacterial
524 communities to an input of HMW organic matter – both in terms of community composition and
525 enzymatic function – varies far more by depth than location, and may be predictable over a
526 regional scale within individual water masses at similar depths.

527 These robust enzymatic patterns may also indicate the ‘value’ of specific substrates to a
528 microbial community in each depth zone. Amendment of epipelagic waters, for example, led to
529 very high α - and β -glucosidase activities, which were higher by several orders of magnitude than
530 rates typically measured in unamended epipelagic waters (Baltar et al., 2009; 2010; Hoarfrost &
531 Arnosti, 2017; Hoarfrost et al., 2019). This pattern suggests that removal of terminal glucose
532 units, whether from polysaccharides, glycosylated proteins, or lipids, may be a critical first step
533 in accessing the complex structures ‘underneath’ (Fig. 5). This feature was also evident during
534 the previous year in epipelagic mesocosms containing water from Stn. 8 (Supplemental
535 Information Fig. S1; Balmonte et al. 2019). Initial removal of terminal glucose and leucine from
536 a HMW substrate may in effect clear the way for activities of a broad range of endopeptidases
537 and polysaccharide hydrolases, which cleave structures mid-chain. The rapid response of the
538 epipelagic community across the entire range of enzyme activities, as well as the high hydrolysis
539 rates triggered by substrate addition, may reflect the fact that microbial communities in
540 epipelagic waters are frequently exposed to freshly produced phytoplankton-derived organic

541 matter rich in amino acids and carbohydrates (Benner et al., 1997; Wakeham et al., 1997; Kaiser
542 & Benner, 2012).

543 The bacterial taxa in epipelagic mesocosms that responded to the addition of HMW
544 organic matter by the 2 d timepoint, in particular increases in the abundance of
545 *Rhodobacteraceae* (*Alphaproteobacteria*) and *Pseudoalteromonadaceae*
546 (*Gammaproteobacteria*) (Fig. 3), also reflect changes in community composition seen in the
547 ocean: bacterial taxa within these classes are usually rare or present in low abundances in
548 seawater, but respond rapidly to seasonal changes in organic matter abundance, such as during
549 phytoplankton blooms (Teeling et al., 2012; Fuhrman et al., 2015; Avcı et al., 2020). We
550 hypothesize that the *Rhodobacteraceae* in particular were likely responding to an increase in low
551 molecular weight substrates that could have been released through the activities of the
552 glucosidases and peptidases, enzymes potentially produced by *Pseudoalteromonadaceae*
553 (Alonso-Sáez et al., 2012; Li et al., 2018).



554

555 **Figure 5.** Conceptual figure illustrates the response of bacterial communities in North Atlantic
 556 epipelagic, mesopelagic, and bathypelagic waters to an input of rapidly sinking, fresh, HMW
 557 organic matter. Community responses depicted here are the timepoint at which significant
 558 responses to the input of HMW organic matter was measured (2 d in epipelagic and mesopelagic
 559 incubations, and 7 d in bathypelagic incubations); polysaccharide hydrolase activities are an
 560 average of all timepoints. Pie charts show the relative contributions of peptidases and
 561 glucosidases (labeled as Pep./Glu.) and polysaccharide hydrolases (labeled as PS Hydro). Glu =
 562 α and β glucosidases, Leu = leucine aminopeptidases, Pep = trypsin and chymotrypsin activities,
 563 Pul = pullulanases, Lam = laminarinases, Xyl = xylanases, Fuc = fucoindanases, Ara =
 564 arabinogalactanases, Chn = chondroitin sulfate hydrolases. The relative abundance of bacterial
 565 communities is illustrated by the three major classes of bacteria that responded to HMW organic
 566 matter input (Alphaproteobacteria, Flavobacteria, and Gammaproteobacteria).

567

568 In mesopelagic mesocosms, the addition of HMW organic matter also produced a broad
569 enzymatic response, consistent with observations of considerable organic matter transformation
570 in this zone (Wakeham et al., 1997; Benner & Amon, 2015). However, mesopelagic mesocosms
571 showed a less robust glucosidase response than epipelagic mesocosms, and were dominated by
572 leucine aminopeptidase, an exo-peptidase activity that may integrate the activities of a range of
573 exopeptidases (Steen et al., 2015) (Fig. 5). Enhancement of rates of peptidase and glucosidase
574 activities were considerably lower than in the epipelagic zone (Fig. 1). The similarities in
575 polysaccharide hydrolase activities in the epipelagic and mesopelagic mesocosms (Fig. 2) may
576 be due in part to convergent trends in bacterial community composition over time (Fig. 4;
577 Supplemental Information S8, S10), since the polysaccharide hydrolase measurements tested the
578 enzymatic responses of microbial communities after they had considerable time to react to
579 substrate addition (Fig. 5). Together, this evidence suggests that mesopelagic communities can
580 respond rapidly to inputs of fresh HMW organic matter, though the rate and spectrum of
581 enzymatic activities differs from those in the epipelagic zone (Fig. 5).

582 The bathypelagic microbial communities responded in a markedly more limited manner.
583 The spectrum of enzyme activities was less broad, and the increases in the rate of enzymatic
584 activities were less substantial and occurred over longer timescales than in epipelagic and
585 mesopelagic communities (Figs. 1, 2). The differences in response times between the amended
586 epipelagic and mesopelagic communities relative to bathypelagic communities may be related in
587 part to differences in the initial size and activity of the heterotrophic bacterial populations. For
588 example, bathypelagic bacterial communities had significantly lower rates of protein production
589 than epipelagic and mesopelagic communities, and protein production rates in amended

590 bathypelagic mesocosms did not increase as quickly as those of mesopelagic and epipelagic
591 communities (Supplemental Fig. S6a). This slower response may suggest that members of these
592 bathypelagic communities were dormant due to limited carbon availability. Fluxes of organic
593 matter that reach the bathypelagic may be sporadic in nature, so bathypelagic communities can
594 enter dormancy until fresh organic matter becomes available, responding even after long periods
595 of starvation (Sebastián et al., 2019). These communities would thus require additional time
596 (relative to epipelagic and mesopelagic communities) to respond to pulses of organic matter,
597 resulting in slower enzymatic responses. Differences in temperature between the incubations
598 (Table 1), may have also played a role in differences in enzymatic activities between the three
599 depths; however, the observation that some enzyme activities were detectable only in amended
600 mesocosms, and others were not detectable at all over the entire time course of the experiments
601 (Figs. 1, 2) suggests that the absence of some enzyme activities in bathypelagic samples is not
602 simply a function of temperature.

603 In bathypelagic mesocosms, increases in bacterial protein production (Supplemental Fig.
604 S6a) and the rates of peptidase and glucosidase activities (Fig. 1) at the 7 d timepoint also
605 corresponded with a shift in bacterial community composition equivalent to that in epipelagic
606 and mesopelagic mesocosms after 2 d (Fig. 4). The substantial decrease in bacterial diversity,
607 richness, and evenness that coincided with this shift in bacterial community composition was
608 likely a result of selection for bacteria capable of degrading HMW organic matter. This shift in
609 community composition resulted in increases in the abundance of *Moritellaceae*
610 (*Gammaproteobacteria*), *Colwelliaceae* (*Gammaproteobacteria*), *Pseudoalteromonadaceae*
611 (*Gammaproteobacteria*), and *Rhodobacteraceae* (*Alphaproteobacteria*), families that had
612 previously been observed responding to the same HMW organic matter in bathypelagic

613 mesocosms (Balmonte et al., 2019). Although these families were present in epipelagic and
614 mesopelagic mesocosms, their response and abundance differed greatly from that in bathypelagic
615 mesocosms, where they became the dominant taxa after the addition of HMW organic matter
616 (Fig. 3). This variability of community composition with depth may account for some of the
617 strong functional differences we observed between distinct bacterial communities, as the ability
618 to produce the enzymes necessary to degrade HMW organic matter varies widely among
619 different bacterial taxa, even those that are closely related (Xing et al., 2015; Saw et al., 2020;
620 Avci et al., 2020).

621 The narrower spectrum of polysaccharide hydrolase activities measured in amended
622 bathypelagic mesocosms suggests that the enzymatic investment to hydrolyze some of the
623 complex structures that were degraded at shallower depths is not likely to pay off for
624 bathypelagic microbial communities. At Stns. 12 and 16, neither fucoidan or arabinogalactan
625 were hydrolyzed, consistent with results from bathypelagic enzyme activities in amended
626 mesocosms from Stn. 8 (Fig. 2; Balmonte et al., 2019). This limited spectrum of extracellular
627 enzymatic activities may reflect their energetic cost-benefit balance – as both arabinogalactan
628 and fucoidan are structurally complex and likely more recalcitrant to microbial degradation
629 (Sichert et al., 2020; Vidal-Melgosa et al., 2021), the cost of enzymatic expression may be too
630 high to justify ‘investment’ in the tools needed to hydrolyze certain structures. Hydrolysis of
631 fucoidan, for example, requires high levels of specialization and energetic investment into
632 hundreds of enzymes (Sichert et al., 2020). If the frequency of encounter with fucoidan in the
633 bathypelagic is low, this strategy may not be productive, as the production of extracellular
634 enzymes is profitable only when the return on investment is sufficient (e.g., Traving et al. 2015).
635 Therefore, the lack of measurable fucoidanase and arabinogalactanase activities in bathypelagic

636 waters suggests that these substrates may not be available in sufficiently high concentrations for
637 production of the required enzymes to pay off. However, the four polysaccharides (pullulan,
638 laminarin, xylan, and chondroitin) that were hydrolyzed in amended bottom water mesocosms
639 represent a breadth and rate of polysaccharide hydrolase activities not typically measurable in
640 bulk incubations of bathypelagic water (Fig. 5; Hoarfrost & Arnosti, 2017; Balmonte et al., 2018;
641 2021). In any case, the enhanced capability of amended bathypelagic microbial communities to
642 degrade complex polysaccharides suggests that an influx of fresh organic matter to the
643 bathypelagic (Broeck et al., 2020; Poff et al., 2021) may fuel the growth of a select set of
644 organisms enzymatically equipped to take advantage of this resource (Fig. 5).

645 Our measurements of depth-related differences in enzymatic activities between distinct
646 microbial communities from the epipelagic, mesopelagic, and bathypelagic in response to an
647 addition of the same HMW organic matter were consistent over a regional scale. The diverse
648 enzymatic responses of epi-, meso-, and bathypelagic microbial communities to inputs of HMW
649 organic matter imply that the structure of HMW organic matter, its residence time at specific
650 depths in the water column, and the distinct enzymatic capabilities of heterotrophic microbial
651 communities at different depths are key factors controlling the ultimate fate of organic matter in
652 the ocean.

653

654 **Data availability**

655 Raw data for peptidase, glucosidase, and polysaccharide hydrolase activities is available through
656 BCO-DMO (<https://www.bco-dmo.org/project/712359>) and 16S rRNA sequence data can be
657 accessed at the NCBI Sequence Read Archive under the accession number PRJNA480640.

658

659 **Author contributions**

660 CA designed the experiments and coordinated work at sea. SB, AH, JB, and SG collected and
661 processed samples at sea and ashore. SB extracted DNA, processed and analyzed the sequence
662 data, and conducted statistical analyses. SB and CA analyzed results, wrote the manuscript, and
663 revised it with input from all co-authors.

664

665 **Competing interests**

666 The authors declare that they have no conflict of interest.

667

668 **Acknowledgements**

669 We thank the captain, crew, and scientific party of the R/V *Endeavor*, cruise EN584. Karylle
670 Abella assisted in sample collection and processing, Dr. John Bane helped to interpret the
671 physiochemical data, and Dr. Jakub Kwintkiewicz aided in library prep and sequencing of the
672 16S rRNA samples. We would also like to thank Dr. James Umbanhowar for his advice on
673 statistical analyses. Funding for this project was provided by NSF (OCE-1332881 and OCE-
674 2022952 to CA).

675

676

677

678

679

680

681

682 **References**

- 683 Alderkamp, A. C., Van Rijssel, M., & Bolhuis, H.: Characterization of marine bacteria and the
684 activity of their enzyme systems involved in degradation of the algal storage glucan
685 laminarin, *FEMS Microbiol. Ecol.*, 59(1), 108-117, 10.1111/j.1574-6941.2006.00219.x,
686 2007.
- 687 Alonso-Sáez, L., Sánchez, O., & Gasol, J. M.: Bacterial uptake of low molecular weight organics
688 in the subtropical Atlantic: Are major phylogenetic groups functionally different?,
689 *Limnol. and Oceanogr.*, 57(3), 798-808, 10.4319/lo.2012.57.3.0798, 2012.
- 690 Amon, R. M., Fitznar, H. P., & Benner, R.: Linkages among the bioreactivity, chemical
691 composition, and diagenetic state of marine dissolved organic matter, *Limnol. and*
692 *Oceanogr.*, 46(2), 287-297, <https://doi.org/10.4319/lo.2001.46.2.0287>, 2001.
- 693 Araki, T., Hashikawa, S., and Morishita, T. (2000). Cloning, sequencing, and expression in *Escherichia*
694 *coli* of the new gene encoding b-1,3-xylanase from a marine bacterium, *Vibrio* sp. Strain XY-
695 214. *Appl. Environ. Microbiol.* 66, 1741-1743.
- 696 Arnosti, C.: Fluorescent derivatization of polysaccharides and carbohydrate-containing
697 biopolymers for measurement of enzyme activities in complex media, *J. Chromatogr.*
698 *B.*, 793(1), 181-191, [https://doi.org/10.1016/S1570-0232\(03\)00375-1](https://doi.org/10.1016/S1570-0232(03)00375-1), 2003.
- 699 Arnosti, C.: Microbial extracellular enzymes and the marine carbon cycle, *Annu. Rev. Mar. Sci.*,
700 3, 401-425, 10.1146/annurev-marine-120709-142731, 2011.
- 701 Arnosti, C., and Repeta, D.J. (1994). Extracellular enzyme activity in anaerobic bacterial cultures:
702 Evidence of pullulanase activity among mesophilic marine bacteria. *Appl. Environ. Microbiol.*
703 60, 840-846.

704 Arnosti, C., Steen, A. D., Ziervogel, K., Ghobrial, S., & Jeffrey, W. H.: Latitudinal gradients in
705 degradation of marine dissolved organic carbon, PLoS One, 6(12), e28900,
706 <https://doi.org/10.1371/journal.pone.0028900>, 2011b.

707 Avci, B., Krüger, K., Fuchs, B. M., Teeling, H., & Amann, R. I.: Polysaccharide niche
708 partitioning of distinct *Polaribacter* clades during North Sea spring algal blooms, ISME
709 J., 14, 1-15, 10.1038/s41396-020-0601-y, 2020.

710 Azam, F.: Microbial control of oceanic carbon flux: the plot thickens, Science, 280(5364), 694-
711 696, 10.1126/science.280.5364.694, 1998.

712 Balmonte, J. P., Buckley, A., Hoarfrost, A., Ghobrial, S., Ziervogel, K., Teske, A., & Arnosti, C.:
713 Community structural differences shape microbial responses to high molecular weight
714 organic matter, Environ. Microbiol., 21, 557-571, 10.1111/1462-2920.14485, 2019.

715 Balmonte, J. P., Simon, M., Giebel, H. A., & Arnosti, C.: A sea change in microbial enzymes:
716 Heterogeneous latitudinal and depth-related gradients in bulk water and particle-
717 associated enzymatic activities from 30° S to 59° N in the Pacific Ocean, Limnol. and
718 Oceanogr., 66(9), 3489-3507, 10.1002/lno.11894, 2021.

719 Balmonte, J. P., Teske, A., & Arnosti, C.: Structure and function of high Arctic pelagic, particle-
720 associated and benthic bacterial communities, Environ. Microbiol., 20(8), 2941-2954,
721 10.1111/1462-2920.14304, 2018.

722 Baltar, F., Aristegui, J., Gasol, J. M., Sintes, E., van Aken, H. M., & Herndl, G. J.: High
723 dissolved extracellular enzymatic activity in the deep central Atlantic Ocean, Aquat.
724 Microb. Ecol., 58(3), 287-302, 10.3354/ame01377, 2010.

725 Baltar, F., Aristegui, J., Sintes, E., Van Aken, H. M., Gasol, J. M., & Herndl, G. J.: Prokaryotic
726 extracellular enzymatic activity in relation to biomass production and respiration in the

727 meso-and bathypelagic waters of the (sub) tropical Atlantic, *Environ. Microbiol.*, 11(8),
728 1998-2014, 10.1111/j.1462-2920.2009.01922.x, 2009.

729 Becker, S., Tebben, J., Coffinet, S., Wiltshire, K., Iversen, M. H., Harder, T., ... & Hehemann, J.
730 H.: Laminarin is a major molecule in the marine carbon cycle, *P. Natl. Acad. Sci. USA*,
731 117(12), 6599-6607, <https://doi.org/10.1073/pnas.1917001117>, 2020.

732 Beier, S., Rivers, A.R., Moran, M.A., and Obernosterer, I.: The transcriptional response of
733 prokaryotes to phytoplankton-derived dissolved organic matter in seawater, *Environ.*
734 *Microbiol.*, 17, 3466-3480, 10.1111/1462-2920.12434, 2015.

735 Benner, R., & Amon, R. M.: The size-reactivity continuum of major bioelements in the ocean,
736 *Annu. Rev. Mar. Sci.*, 7, 185-205, 10.1146/annurev-marine-010213-135126, 2015.

737 Benner, R., Biddanda, B., Black, B., & McCarthy, M.: Abundance, size distribution, and stable
738 carbon and nitrogen isotopic compositions of marine organic matter isolated by
739 tangential-flow ultrafiltration, *Mar. Chem.*, 57(3-4), 243-263, 10.1016/S0304-
740 4203(97)00013-3, 1997.

741 Bolyen, E., Rideout, J. R., Dillon, M. R., Bokulich, N. A., Abnet, C., Al-Ghalith, G. A., ... & Bai,
742 Y.: Reproducible, interactive, scalable and extensible microbiome data using QIIME 2,
743 *Nat. Biotechnol.*, 37, 852-857, <https://doi.org/10.1038/s41587-019-0209-9>, 2019.

744 Broek, T. A. B. *et al*: Low molecular weight dissolved organic carbon: aging, compositional
745 changes, and selective utilization during global ocean circulation, *Global Biogeochem.*
746 *Cycles*, 34, e2020GB006547, 10.1029/2020GB006547, 2020.

747 Callahan, B. J., McMurdie, P. J., Rosen, M. J., Han, A. W., Johnson, A. J. A., & Holmes, S. P.:
748 DADA2: high-resolution sample inference from Illumina amplicon data, *Nat. Methods*,
749 13(7), 581, 10.1038/nmeth.3869, 2016

750 DeLong, E. F., Preston, C. M., Mincer, T., Rich, V., Hallam, S. J., Frigaard, N. U., ... &
751 Chisholm, S. W.: Community genomics among stratified microbial assemblages in the
752 ocean's interior, *Science*, 311(5760), 496-503, 10.1126/science.1120250, 2006.

753 Fuhrman, J. A., Cram, J. A., & Needham, D. M.: Marine microbial community dynamics and
754 their ecological interpretation, *Nat. Rev. Microbiol.*, 13(3), 133-146,
755 10.1038/nmeth.3869, 2015.

756 Guerrero-Feijóo, E., Nieto-Cid, M., Sintés, E., Dobal-Amador, V., Hernando-Morales, V.,
757 Álvarez, M., ... & Varela, M. M.: Optical properties of dissolved organic matter relate to
758 different depth-specific patterns of archaeal and bacterial community structure in the
759 North Atlantic Ocean, *FEMS Microbiol. Ecol.*, 93(1), fiw224, 10.1093/femsec/fiw224,
760 2016.

761 Hartley, B., Barber, H. G., Carter, J. R., Sims, P. A.: An atlas of British diatoms, Balogh
762 Scientific Books, 1996.

763 Hedges, J.I., Baldock, J.A., Gelinás, Y., Lee, C., Peterson, M., and Wakeham, S.G.: Evidence for non-
764 selective preservation of organic matter in sinking particles. *Nature* 409, 801-804, 2001.

765 Heiderich, J., & Todd, R. E.: Along-stream evolution of Gulf Stream volume transport. *J. Phys.*
766 *Oceanogr.*, 50(8), 2251-2270, 10.1175/JPO-D-19-0303.1, 2020.

767 Hoarfrost, A., & Arnosti, C.: Heterotrophic Extracellular Enzymatic Activities in the Atlantic
768 Ocean Follow Patterns Across Spatial and Depth Regimes, *Frontiers Mar. Sci.*, 4, 200,
769 10.3389/fmars.2017.00200, 2017.

770 Hoarfrost, A., Balmonte, J. P., Ghobrial, S., Ziervogel, K., Bane, J., Gawarkiewicz, G., &
771 Arnosti, C.: Gulf Stream ring water intrusion on the Mid-Atlantic Bight continental shelf

772 break affects microbially-driven carbon cycling, *Frontiers Mar. Sci.*, 6, 394,
773 10.3389/fmars.2019.00394, 2019.

774 Hoppe, H. G.: Significance of exoenzymatic activities in the ecology of brackish water:
775 measurements by means of methylumbelliferyl-substrates, *Marine Ecol. Prog. Ser.*, 299-
776 308, <https://www.jstor.org/stable/44634717>, 1983.

777 Hothorn, T., Bretz, F., & Westfall, P.: Simultaneous inference in general parametric models,
778 *Biometrical J.*, 50(3), 346-363, 10.1002/bimj.200810425, 2008

779 Kaiser, K., & Benner, R.: Organic matter transformations in the upper mesopelagic zone of the
780 North Pacific: Chemical composition and linkages to microbial community structure, *J.*
781 *Geophys. Res-Oceans*, 117(C1), 10.1029/2011JC007141, 2012.

782 Kirchman, D.: Measuring bacterial biomass production and growth rates from leucine
783 incorporation in natural aquatic environments, *Method Microbiol.*, 30, 227–237,
784 [https://doi.org/10.1016/S0580-9517\(01\)30047-8](https://doi.org/10.1016/S0580-9517(01)30047-8), 2001.

785 Kirchman, D., K'Neas, E., and Hodson, R.: Leucine incorporation and its potential as a measure
786 of protein synthesis by bacteria in natural aquatic systems, *Appl. Environ. Microbiol.*, 49,
787 599-607, 10.1128/aem.49.3.599-607.1985, 1985.

788 Li, D. X., Zhang, H., Chen, X. H., Xie, Z. X., Zhang, Y., Zhang, S. F., ... & Wang, D. Z.:
789 Metaproteomics reveals major microbial players and their metabolic activities during the
790 blooming period of a marine dinoflagellate *Prorocentrum donghaiense*, *Environ.*
791 *Microbiol.*, 20(2), 632-644, 10.1111/1462-2920.13986, 2018.

792 Luria, C. M., Amaral-Zettler, L. A., Ducklow, H. W., Repeta, D. J., Rhyne, A. L., & Rich, J. J.:
793 Seasonal shifts in bacterial community responses to phytoplankton-derived dissolved

794 organic matter in the Western Antarctic Peninsula, *Frontiers Microbiol.*, 8, 2117,
795 10.3389/fmicb.2017.02117, 2017.

796 Martinez Arbizu, P. (2019). pairwiseAdonis: Pairwise multilevel comparison using adonis. R
797 package version 0.3. <https://github.com/pmartinezarbizu/pairwiseAdonis>

798 Martin, M.: Cutadapt removes adapter sequences from high-throughput sequencing reads,
799 *EMBnet. J.*, 17(1), pp-10, 2011.

800 McMurdie, P. J., & Holmes, S.: phyloseq: An R package for reproducible interactive analysis
801 and graphics of microbiome census data, *PloS one*, 8(4), e61217,
802 10.1371/journal.pone.0061217, 2013.

803 Mestre, M., Ruiz-González, C., Logares, R., Duarte, C. M., Gasol, J. M., & Sala, M. M.: Sinking
804 particles promote vertical connectivity in the ocean microbiome, *P. Natl. A. Sci.*
805 *USA*, 115(29), E6799-E6807, 10.1073/pnas.1802470115, 2018.

806 Oksanen, J., Blanchet, F. G., Friendly, M., Kindt, R., Legendre, P., McGlenn, D., Minchin, P. R.,
807 O'Hara, R. B., Simpson, G. L., Solymos, R., Stevens, M. H. H., Szoecs, E., Wagner, H.:
808 vegan: Community Ecology Package, R package version 2.4-6, [https://CRAN.R-](https://CRAN.R-project.org/package=vegan)
809 [project.org/package=vegan](https://CRAN.R-project.org/package=vegan), 2018.

810 Pinheiro J, Bates D, DebRoy S, Sarkar D and R Core Team: nlme: Linear and Nonlinear Mixed
811 Effects Models, R package version 3.1-137, <https://CRAN.R-project.org/package=nlme>,
812 2018.

813 Poff, K. E., Leu, A. O., Eppley, J. M., Karl, D. M., & DeLong, E. F.: Microbial dynamics of
814 elevated carbon flux in the open ocean's abyss, *P. Natl. Acad. Sci-Biol.*, 118(4),
815 e2018269118, 10.1073/pnas.2018269118, vci 2021.

816 Pruesse, E., Quast, C., Knittel, K., Fuchs, B. M., Ludwig, W., Peplies, J., & Glöckner, F. O.:
817 SILVA: a comprehensive online resource for quality checked and aligned ribosomal
818 RNA sequence data compatible with ARB, *Nucleic Acids Res.*, 35(21), 7188-7196,
819 10.1093/nar/gkm864, 2007.

820 R Core Team: R: A language and environment for statistical computing, R Foundation for
821 Statistical Computing, Vienna, Austria, URL <https://www.R-project.org/>, 2017.

822 Ruiz-González C, Mestre M, Estrada M, Sebastián M, Salazar G, Agustí S, Moreno-Ostos E,
823 Reche I, Álvarez-Salgado XA, Morán XA, Duarte CM: Major imprint of surface
824 plankton on deep ocean prokaryotic structure and activity, *Mol. Ecol.*, 29(10):1820-38,
825 10.1111/mec.15454 2020.

826 Saw, J. H., Nunoura, T., Hirai, M., Takaki, Y., Parsons, R., Michelsen, M., ... & Carlson, C. A.:
827 Pangenomics Analysis Reveals Diversification of Enzyme Families and Niche
828 Specialization in Globally Abundant SAR202 Bacteria, *mBio*, 11(1),
829 10.1128/mBio.02975-19, 2020.

830 Schlitzer, R.: Data Analysis and Visualization with Ocean Data View, *CMOS Bulletin SCMO*,
831 43 (1), pp. 9-13, 2015.

832 Sebastián, M., Estrany, M., Ruiz-González, C., Forn, I., Sala, M. M., Gasol, J. M., & Marrasé,
833 C.: High growth potential of long-term starved deep ocean opportunistic heterotrophic
834 bacteria, *Front. Microbiol.*, 10, 760, <https://doi.org/10.3389/fmicb.2019.00760>, 2019.

835 Sebastián, M., Forn, I., Auladell, A., Gómez-Letona, M., Sala, M. M., Gasol, J. M., & Marrasé,
836 C.: Differential recruitment of opportunistic taxa leads to contrasting abilities in carbon
837 processing by bathypelagic and surface microbial communities, *Environ.*
838 *Microbiol.*, 23(1), 190-206, 10.1111/1462-2920.15292, 2021.

839 Sichert, A., Corzett, C. H., Schechter, M. S., Unfried, F., Markert, S., Becher, D., ... &
840 Hehemann, J. H.: Verrucomicrobia use hundreds of enzymes to digest the algal
841 polysaccharide fucoidan, *Nat. Microbiol.*, 5(8), 1026-1039, [https://doi-](https://doi-org.libproxy.lib.unc.edu/10.1038/s41564-020-0720-2)
842 [org.libproxy.lib.unc.edu/10.1038/s41564-020-0720-2](https://doi-org.libproxy.lib.unc.edu/10.1038/s41564-020-0720-2), 2020.

843 Simon, M., & Azam, F.: Protein content and protein synthesis rates of planktonic marine
844 bacteria, *Miar. Ecol. Prog. Ser.*, 51:201–213, 1989.

845 Steen, A. D., Vazin, J. P., Hagen, S. M., Mulligan, K. H., & Wilhelm, S. W.: Substrate
846 specificity of aquatic extracellular peptidases assessed by competitive inhibition assays
847 using synthetic substrates, *Aquat. Microb. Ecol.*, 75(3), 271-281, 10.3354/ame01755,
848 2015.

849 Steen, A. D., Ziervogel, K., Ghobrial, S., & Arnosti, C.: Functional variation among
850 polysaccharide-hydrolyzing microbial communities in the Gulf of Mexico, *Mar. Chem.*,
851 138, 13-20, 10.1016/j.marchem.2012.06.001, 2012.

852 Sunagawa, S., Coelho, L. P., Chaffron, S., Kultima, J. R., Labadie, K., Salazar, G., ... & Cornejo-
853 Castillo, F. M.: Structure and function of the global ocean microbiome, *Science*,
854 348(6237), 1261359, 10.1126/science.1261359, 2015.

855 Talley, L. D.: *Descriptive physical oceanography: an introduction*, Academic press, 2011.

856 Teeling, H., Fuchs, B. M., Becher, D., Klockow, C., Gardebrecht, A., Bennke, C. M., ... &
857 Weber, M.: Substrate-controlled succession of marine bacterioplankton populations
858 induced by a phytoplankton bloom, *Science*, 336(6081), 608-611,
859 10.1126/science.1218344, 2012.

860 Teeling, H., Fuchs, B. M., Bennke, C. M., Krueger, K., Chafee, M., Kappelmann, L., ... & Lucas,
861 J.: Recurring patterns in bacterioplankton dynamics during coastal spring algae blooms,
862 *Elife*, 5, 10.7554/eLife.11888, 2016.

863 Traving, S. J., Thygesen, U. H., Riemann, L., & Stedmon, C. A.: A model of extracellular
864 enzymes in free-living microbes: which strategy pays off?, *Appl. Environ.*
865 *Microb.*, 81(21), 7385-7393, 10.1128/AEM.02070-15, 2015.

866 Vidal-Melgosa, S., Sichert, A., Francis, T. B., Bartosik, D., Niggemann, J., Wichels, A., ... &
867 Hehemann, J. H.: Diatom fucan polysaccharide precipitates carbon during algal blooms.
868 *Nat. Commun.*, 12(1), 1-13, [https://doi-org.libproxy.lib.unc.edu/10.1038/s41467-021-](https://doi-org.libproxy.lib.unc.edu/10.1038/s41467-021-21009-6)
869 [21009-6](https://doi-org.libproxy.lib.unc.edu/10.1038/s41467-021-21009-6), 2021.

870 Wakeham, S. G., Lee, C., Hedges, J. I., Hernes, P. J., & Peterson, M. J.: Molecular indicators of
871 diagenetic status in marine organic matter, *Geochim. Cosmochim. Ac.*, 61(24), 5363-
872 5369, 10.1016/S0016-7037(97)00312-8, 1997.

873 Wegner, C.-E., Richter-Heitmann, T., Klindworth, A., Klockow, C., Richter, M., Achstetter, T.,
874 Glockner, F.O., and Harder, J. (2013). Expression of sulfatases in *Rhodopirellula baltica* and the
875 diversity of sulfatases in the genus *Rhodopirellula*. *Marine Genomics* 9.

876 Weiss, M. S., Abele, U., Weckesser, J., Welte, W. U., Schiltz, E., & Schulz, G. E.: Molecular
877 architecture and electrostatic properties of a bacterial porin, *Science*, 254(5038), 1627-
878 1630, 10.1126/science.1721242, 1991.

879 Xing, P., Hahnke, R. L., Unfried, F., Markert, S., Huang, S., Barbeyron, T., ... & Amann, R. I.:
880 Niches of two polysaccharide-degrading *Polaribacter* isolates from the North Sea during
881 a spring diatom bloom, *ISME J.*, 9(6), 1410, 10.1038/ismej.2014.225, 2015.